

## Supporting Information

### **Cellulose Benzoate Synthesis *via* Homogeneous Transesterification Catalyzed by Superbase-Derived Ionic Liquids for Advanced Applications**

Yuhui Ci,<sup>a</sup> Xiangjian Yang,<sup>a</sup> Yunqian Ma,<sup>b</sup> Feng Xu<sup>\*c</sup> and Yanjun Tang<sup>\*a</sup>

<sup>a</sup> National Engineering Laboratory of Textile Fiber Materials and Processing Technology, Zhejiang Sci-Tech University, Hangzhou, 310018, P. R. China.

<sup>b</sup> Longzihu New Energy Laboratory, Zhengzhou Institute of Emerging Industrial Technology, Henan University, Zhengzhou 450000, P. R. China

<sup>c</sup> Beijing Key Laboratory of Lignocellulosic Chemistry, Beijing Forestry University, Beijing, 100083, P. R. China.

\*Corresponding author:

Email address: [xfx315@bjfu.edu.cn](mailto:xfx315@bjfu.edu.cn) (F. Xu), [tangyj@zstu.edu.cn](mailto:tangyj@zstu.edu.cn) (Y. J. Tang)

Note S1. Density functional theory calculations.....	3
Table S1. DS and solubility of cellulose benzoate prepared by transesterification under different conditions. ....	5
Table S2. Preparation conditions for PVDF/cellulose benzoate electrospun membranes. ....	6
Table S3. Comparison of different membrane materials for oil/water emulsion separation. ....	7
Table S4. Preparation conditions, Bulk density and BET surface area of aerogel.	8
Table S5. Thermal behavior data of cellulose and cellulose benzoate samples with varying degrees of substitution. ....	9
Fig. S1. SEM images of PVDF/cellulose benzoate electrospun membranes for oil-water separation, along with the fiber diameter distribution for each sample. ....	10
Fig. S2. (a) Oil-water separation device and the oil droplet size distribution of the emulsion (b) before and (c) after separation. ....	11
Fig. S3. The FT-IR spectrum of aerogel and sample 5 .....	12
Fig. S4 <sup>1</sup> H NMR spectrum of fresh [DBUH]Lev/DMSO, vinyl benzoate, and recycled [DBUH]Lev/DMSO. ....	13
Fig. S5 <sup>13</sup> C NMR spectrum of fresh [DBUH]Lev/DMSO, vinyl benzoate, and recycled [DBUH]Lev/DMSO. ....	14
References .....	15

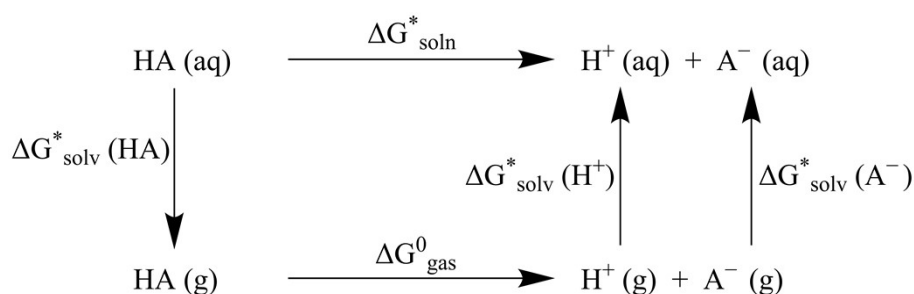
## Note S1. Density functional theory calculations

All of the calculations were conducted using Gaussian 16 programs<sup>1</sup>. Wave function analysis was performed using the multiwfn 3.8 dev program<sup>2</sup> and visualization was performed using VMD 1.9.3 software<sup>3</sup>.

### Calculation process of solvation free energy

1. Geometry optimization and frequency analysis were performed for structure (1) based on the SMD implicit solvent model at the B3LYP-D3 (BJ)/6-311G (d) level<sup>4-7</sup>.
2. The electronic energies of structure (1) were calculated at the B2PLYP-D3/def2-TZVP level<sup>8-10</sup>. The gas-phase free energy ( $\Delta_{\text{gas}}$ ) was determined using Shermo software, with a zero-point energy (ZPE) correction factor of 0.9882<sup>11</sup> at the B3LYP-D3 (BJ)/6-311G (d) level<sup>4-7</sup>.
3. The vacuum electron energies for structure (1) were calculated at the M05-2X/6-31G (d) level<sup>12, 13</sup>.
4. The electronic energies of structure (1) in the solvent environment were calculated at the M05-2X/6-31G (d) level<sup>12, 13</sup> based on the SMD implicit solvent model.

### Calculation of pKa



According to the above thermodynamic cycle<sup>14</sup>, the calculation formula of pKa is as follows:

$$\Delta G_{\text{soln}} = \Delta G_{\text{gas}} + \Delta G_{\text{solv}}(\text{H}^+) + \Delta G_{\text{solv}}(\text{A}^-) - \Delta G_{\text{solv}}(\text{HA}) \quad (1)$$

$$\text{pK}_a = \frac{\Delta G_{\text{soln}}^*}{RT \ln 10} \quad (2)$$

$$\Delta G_{\text{soln}}^* = \Delta G_{\text{soln}} + \Delta n \times 1.89 \quad (3)$$

Based on the studies of Dixon et al.<sup>15</sup>, the solvation free energy of H<sup>+</sup> was calculated using explicit and implicit solvent models at the B3LYP-D3(BJ)/6-311++G (d, p) level<sup>4-6, 16</sup>. The solvation free energy of H<sup>+</sup> in DMSO and DMF is consistent with previous reports<sup>17, 18</sup>.

### Transition state search

Geometry optimizations and frequency calculations were carried out at the B3LYP-D3 (BJ)/6-311G (d) level<sup>4-7</sup> using the SMD implicit solvent model. After convergence, frequency calculations were performed at the same level to classify stationary points as minima or transition states, identified by unique imaginary frequencies. The intrinsic reaction coordinate (IRC) calculations were subsequently performed to confirm that the transition structure connected the relevant reactants and products. Stationary point electronic energies were calculated at the PWPB95-D3 (BJ)/def2-TZVPP level<sup>5, 6, 8-10</sup> using the ORCA 5.0 program<sup>19</sup>. The SMD parameter settings for [DBUH]Lev are based on the SMD-GIL (generic ionic liquid) model proposed by Truhlar et al.<sup>20</sup>. Reaction rate constant was calculated using the TST calculator developed by Lu<sup>21</sup> and fitted to the Arrhenius curve using the following equation:

$$k = Ae^{-\frac{E_a}{RT}} \quad (4)$$

where k is the reaction rate constant, A is the pre-exponential factor (frequency factor), E<sub>a</sub> is the activation energy, R is the universal gas constant, and T is the absolute temperature in Kelvin.

**Table S1. DS and solubility of cellulose benzoate prepared by transesterification under different conditions.**

	Temperature (°C)	Time (h)	AGU:VB	Solvent	DS	Solubility <sup>a</sup>	
						DMSO	CHCl <sub>3</sub>
1	40	4	1:6	[DBUH]Lev/DMSO	0.93	+	+
2	60	4	1:6	[DBUH]Lev/DMSO	1.78	+	+
3	80	4	1:6	[DBUH]Lev/DMSO	2.91	+	+
4	100	4	1:6	[DBUH]Lev/DMSO	2.59	+	+
5	80	1	1:6	[DBUH]Lev/DMSO	1.10	+	+
6	80	2	1:6	[DBUH]Lev/DMSO	2.13	+	+
7	80	6	1:6	[DBUH]Lev/DMSO	2.68	+	+
8	80	4	1:1	[DBUH]Lev/DMSO	1.64	+	+
9	80	4	1:3	[DBUH]Lev/DMSO	2.85	+	+
10	80	4	1:9	[DBUH]Lev/DMSO	2.44	+	+
11	80	4	1:6	[DBUH]Lev/DMF	2.64	+	+
12	80	4	1:6	[DBUH]Lev/DMAc	2.09	+	+
13	80	4	1:6	[DBUH]Lev	1.42	+	+

**Note:** The concentration of MCC was 5 wt%, and the amount of co-solvent was 40 wt%.

<sup>a</sup> Insoluble (–) and soluble (+) in different solvents.

**Table S2. Preparation conditions for PVDF/cellulose benzoate electrospun membranes.**

	<b>Acetone (g)</b>	<b>DMF (g)</b>	<b>PVDF (g)</b>	<b>CB (g)</b>
1	5.4	12.6	2.00	0
2	5.4	12.6	1.90	0.10
3	5.4	12.6	1.80	0.20
4	5.4	12.6	1.70	0.30
5	5.4	12.6	1.60	0.40

**Table S3. Comparison of different membrane materials for oil/water emulsion separation.**

Material	Flux ( $L \cdot m^{-2} \cdot h^{-1}$ )	Separation efficiency (%)	Ref.
PVDF-g-AAc (nonsolvent induced phase separation)	300	90	22
GO/PDA/MCEM	146	96%	23
Polysulfone/PEG	120	>95%	24
PVA/graphene oxide	102-610	>93.5%	25
Ceramic ( $\alpha$ -Al <sub>2</sub> O <sub>3</sub> -ZrO <sub>2</sub> )	40-80	>90%	26
PVDF-DTPA/MWCNT/TiO	943.6	>97.4%	27
Poly (p-phenylene sulfide)	154.95	98.98	28
PVDF/MWCNTs	700	>90%	29
Cellulose benzoate/PVDF	210-720	>96%	This work

**Table S4. Preparation conditions, Bulk density and BET surface area of aerogel.**

	<b>DMSO (g)</b>	<b>CB (g)</b>	<b>TDI (mL)</b>	<b>Catalyst (<math>\mu\text{L}</math>)</b>	<b>Bulk density (<math>\text{g}/\text{cm}^3</math>)</b>	<b>S<sub>BET</sub> (<math>\text{m}^2/\text{g}</math>)</b>
1	9.9	0.1	0.2	10	0.0587	0.775
2	9.8	0.2	0.4	10	0.1369	4.132
3	9.7	0.3	0.6	10	0.2260	1.277
4	9.6	0.4	0.8	10	0.3101	0.668
5	9.5	0.5	1.0	10	/	/



**Table S5. Thermal behavior data of cellulose and cellulose benzoate samples with varying degrees of substitution.**

Sample	DS	TG <sub>-5%</sub>	TG <sub>p</sub>	T <sub>g</sub>	Residue
Original	/	285.85 °C	352.95 °C	/	6.22%
3	2.91	338.19 °C	373.49 °C	176.90 °C	7.60%
6	2.13	333.34 °C	367.34 °C	177.27 °C	7.36%
5	1.10	332.97 °C	370.57 °C	178.55 °C	6.81%

**Fig. S1. SEM images of PVDF/cellulose benzoate electrospun membranes for oil-water separation, along with the fiber diameter distribution for each sample.**

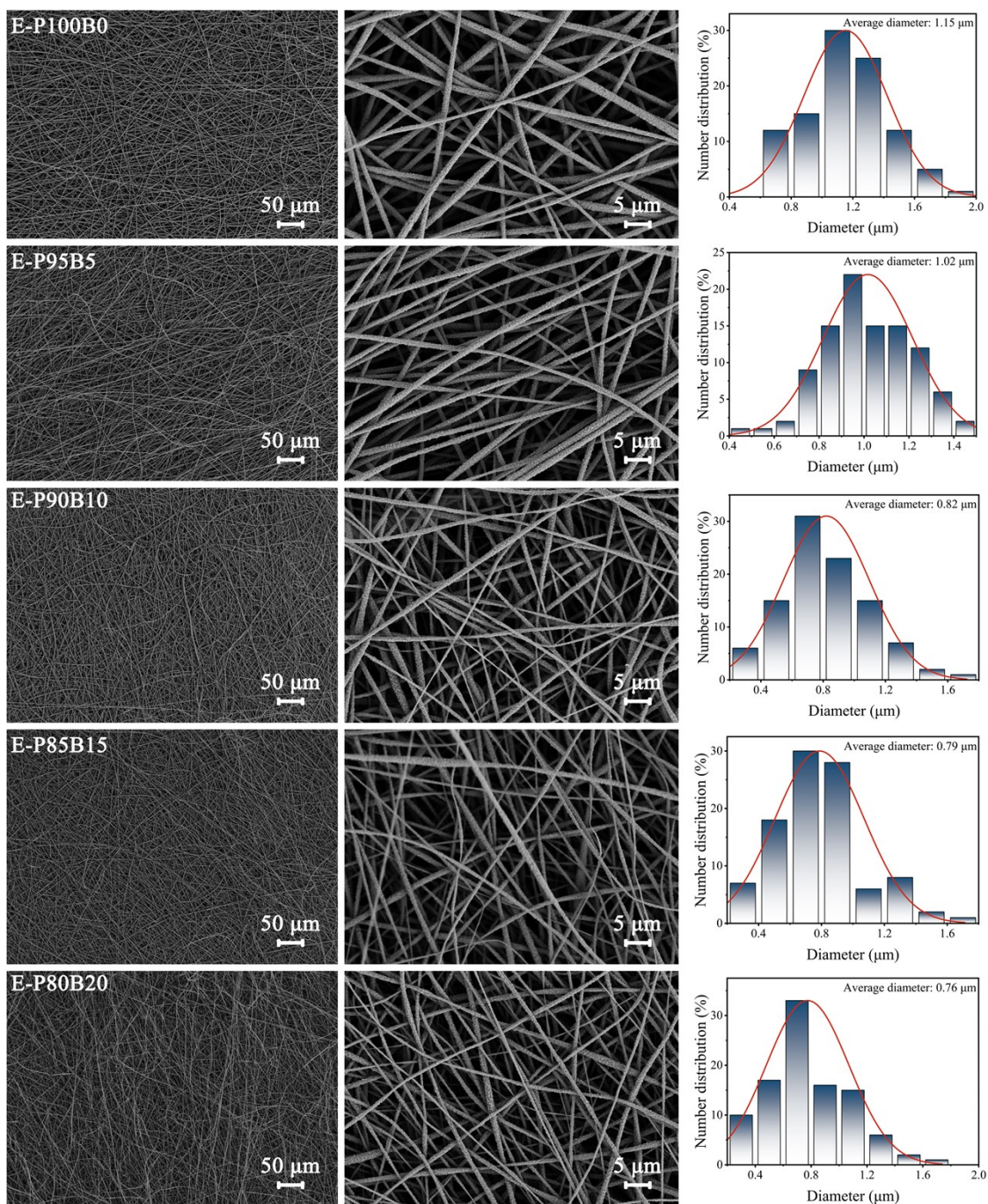


**Fig. S2. (a) Oil-water separation device and the oil droplet size distribution of the emulsion (b) before and (c) after separation.**

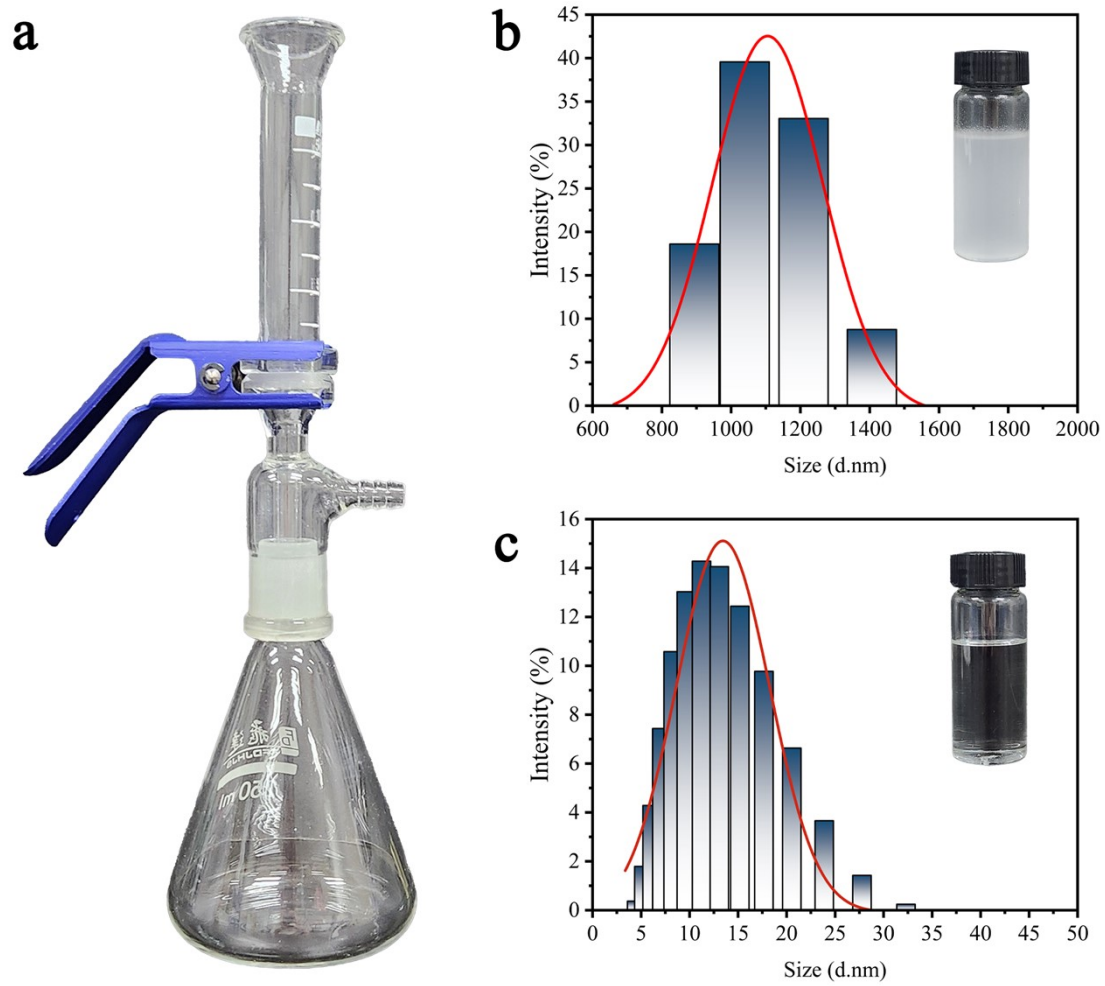


Fig. S3. The FT-IR spectrum of aerogel and sample 5

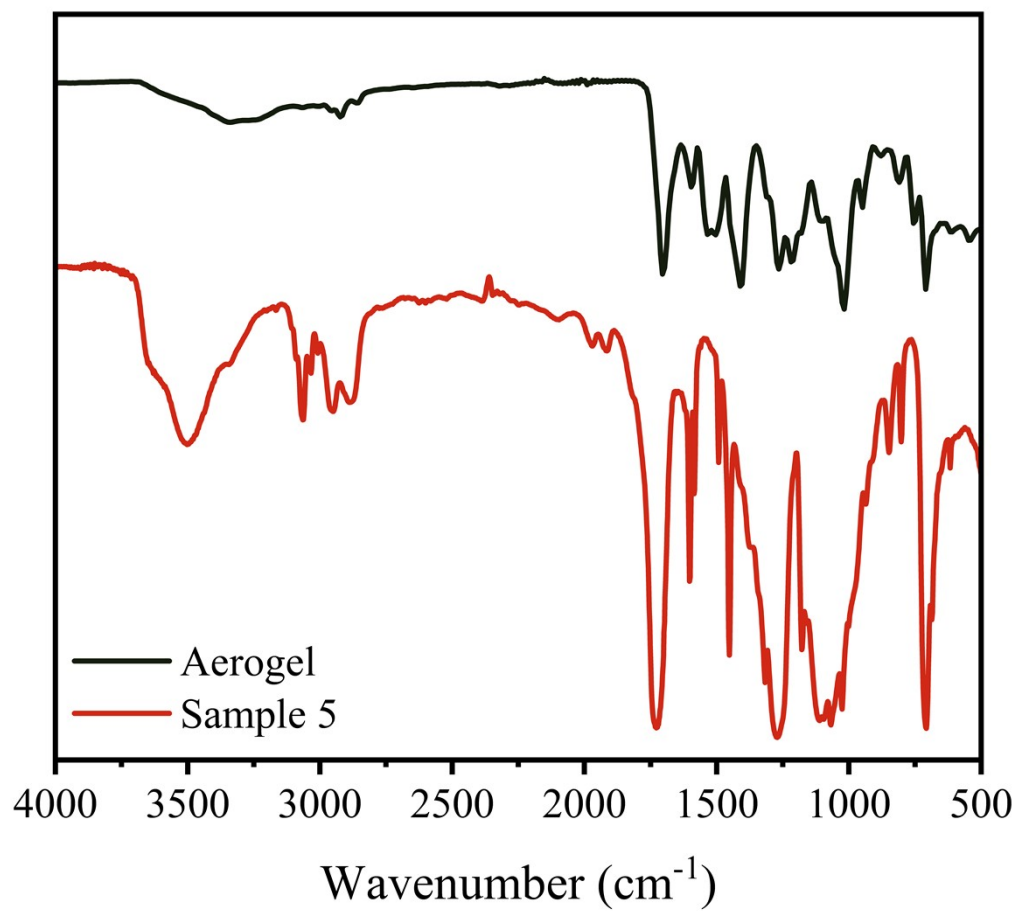
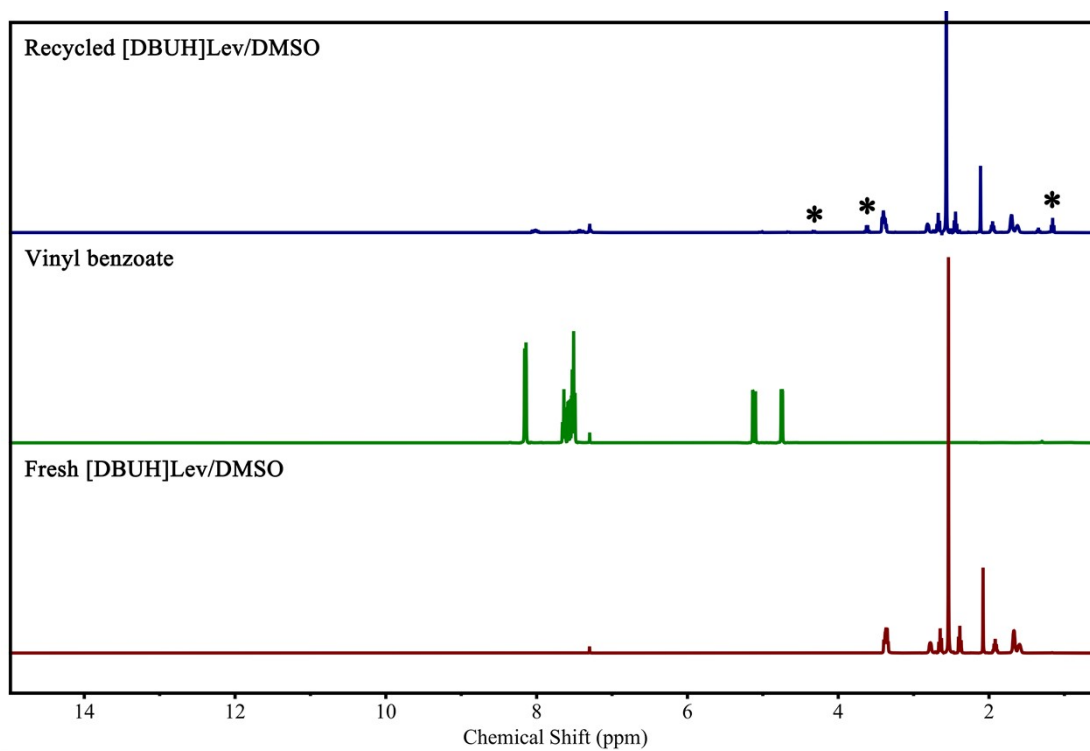
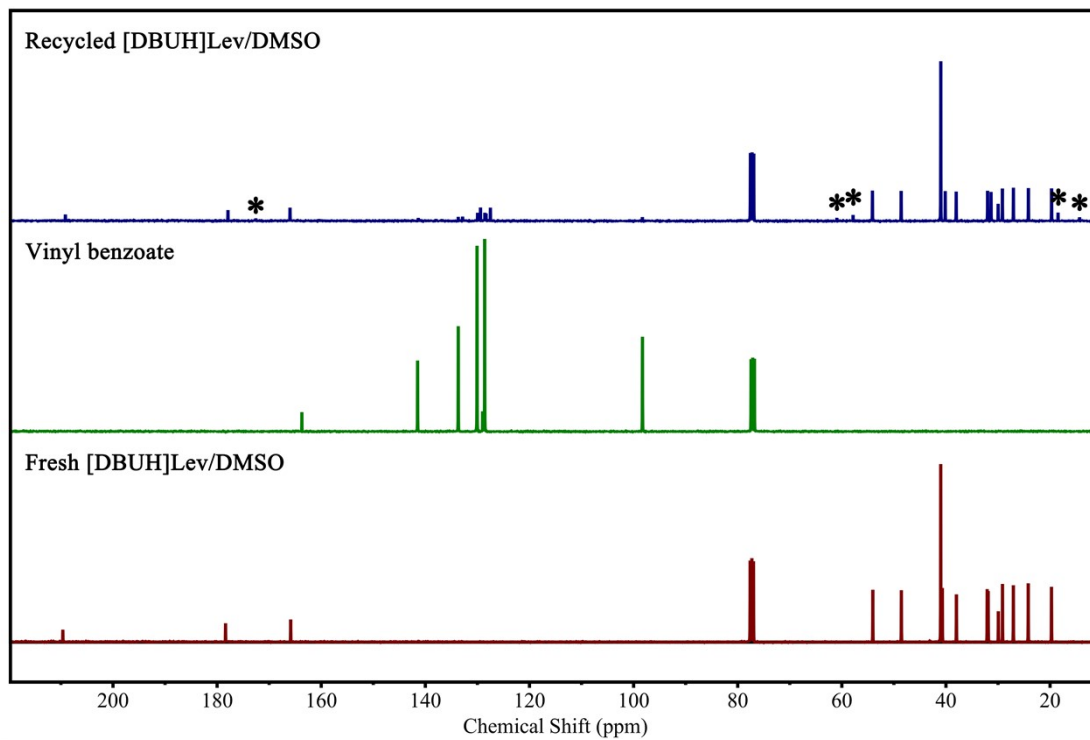


Fig. S4  $^1\text{H}$  NMR spectrum of fresh [DBUH]Lev/DMSO, vinyl benzoate, and recycled [DBUH]Lev/DMSO.



The symbol \* refers to peaks due to impurities.

Fig. S5  $^{13}\text{C}$  NMR spectrum of fresh [DBUH]Lev/DMSO, vinyl benzoate, and recycled [DBUH]Lev/DMSO.



The symbol \* refers to peaks due to impurities.

## References

1. M. J. Frisch, G. W. Trucks, H. B. Schlegel, G. E. Scuseria, M. A. Robb, J. R. Cheeseman, G. Scalmani, V. Barone, G. A. Petersson, H. Nakatsuji, X. Li, M. Caricato, A. V. Marenich, J. Bloino, B. G. Janesko, R. Gomperts, B. Mennucci, H. P. Hratchian, J. V. Ortiz, A. F. Izmaylov, J. L. Sonnenberg, Williams, F. Ding, F. Lipparini, F. Egidi, J. Goings, B. Peng, A. Petrone, T. Henderson, D. Ranasinghe, V. G. Zakrzewski, J. Gao, N. Rega, G. Zheng, W. Liang, M. Hada, M. Ehara, K. Toyota, R. Fukuda, J. Hasegawa, M. Ishida, T. Nakajima, Y. Honda, O. Kitao, H. Nakai, T. Vreven, K. Throssell, J. A. Montgomery Jr., J. E. Peralta, F. Ogliaro, M. J. Bearpark, J. J. Heyd, E. N. Brothers, K. N. Kudin, V. N. Staroverov, T. A. Keith, R. Kobayashi, J. Normand, K. Raghavachari, A. P. Rendell, J. C. Burant, S. S. Iyengar, J. Tomasi, M. Cossi, J. M. Millam, M. Klene, C. Adamo, R. Cammi, J. W. Ochterski, R. L. Martin, K. Morokuma, O. Farkas, J. B. Foresman and D. J. Fox, *Journal*, 2016.
2. T. Lu and F. Chen, *Journal of computational chemistry*, 2012, **33**, 580-592.
3. W. Humphrey, A. Dalke and K. Schulten, *Journal of molecular graphics*, 1996, **14**, 33-38.
4. P. J. Stephens, F. J. Devlin, C. F. Chabalowski and M. J. Frisch, *The Journal of Physical Chemistry*, 1994, **98**, 11623-11627.
5. E. R. Johnson and A. D. Becke, *Chemical physics letters*, 2006, **432**, 600-603.
6. S. Grimme, J. Antony, S. Ehrlich and H. Krieg, *The Journal of chemical physics*, 2010, **132**.
7. R. Krishnan, J. S. Binkley, R. Seeger and J. A. Pople, *The Journal of chemical physics*, 1980, **72**, 650-654.
8. L. Goerigk and S. Grimme, *Journal of Chemical Theory and Computation*, 2011, **7**, 291-309.
9. F. Weigend and R. Ahlrichs, *Physical Chemistry Chemical Physics*, 2005, **7**, 3297-3305.
10. F. Weigend, *Physical Chemistry Chemical Physics*, 2006, **8**, 1057-1065.
11. J. P. Merrick, D. Moran and L. Radom, *The Journal of Physical Chemistry A*, 2007, **111**, 11683-11700.
12. Y. Zhao, N. E. Schultz and D. G. Truhlar, *Journal of Chemical Theory and Computation*, 2006, **2**, 364-382.
13. P. C. Hariharan and J. A. Pople, *Theoretica chimica acta*, 1973, **28**, 213-222.
14. M. D. Liptak and G. C. Shields, *Journal of the American Chemical Society*, 2001, **123**, 7314-7319.
15. C.-G. Zhan and D. A. Dixon, *The Journal of Physical Chemistry A*, 2001, **105**, 11534-11540.
16. G. A. Petersson and M. A. Al-Laham, *The Journal of chemical physics*, 1991, **94**, 6081-6090.
17. Z. Marković, J. Tošović, D. Milenković and S. Marković, *Computational and Theoretical Chemistry*, 2016, **1077**, 11-17.
18. J. Rimarčík, V. Lukeš, E. Klein and M. Ilčin, *Journal of Molecular Structure: THEOCHEM*, 2010, **952**, 25-30.
19. F. Neese, *WIREs Computational Molecular Science*, 2022, **12**, e1606.

20. V. S. Bernales, A. V. Marenich, R. Contreras, C. J. Cramer and D. G. Truhlar, *The Journal of Physical Chemistry B*, 2012, **116**, 9122-9129.
21. L. Tian, TSTcalculator, (<http://sobereva.com/310>).
22. L. Wang, K. Pan, L. Li and B. Cao, *Ind. Eng. Chem. Res.*, 2014, **53**, 6401-6408.
23. Z. Liu, W. Wu, Y. Liu, C. Qin, M. Meng, Y. Jiang, J. Qiu and J. Peng, *Sep. Purif. Technol.*, 2018, **199**, 37-46.
24. T. Yuan, J. Meng, T. Hao, Y. Zhang and M. Xu, *J. Membr. Sci.*, 2014, **470**, 112-124.
25. D. Qin, Z. Liu, H. Bai, D. D. Sun and X. Song, *Sci. Rep.*, 2016, **6**, 24365.
26. J. Milić, I. Petrinić, A. Goršek and M. Simonič, *Open Chemistry*, 2014, **12**, 242-249.
27. K. Venkatesh, G. Arthanareeswaran, A. Chandra Bose, P. Suresh Kumar and J. Kweon, *Sep. Purif. Technol.*, 2021, **257**, 117926.
28. Y. Gao, Z. Li, B. Cheng and K. Su, *Sep. Purif. Technol.*, 2018, **192**, 262-270.
29. A. Moslehyani, A. F. Ismail, M. H. D. Othman and T. Matsuura, *Desalination*, 2015, **363**, 99-111.